China Geology 1 (2019) 40–48

China Geology

Journal homepage: http://chinageology.cgs.cn

# Distribution of potential geological hazards and control factors in Qingdao offshore, China

Ze Ning[a, b, c,*], Man-man Lin[d], Yong Zhang[a, b,*], Xiao-bo Zhang[a, b], Xiang-huai Kong[a, b]

[a] *Qingdao Institute of Marine Geology, China Geology Survey, Ministry of Natural Resources, Qingdao* 266071, *China*
[b] *Laboratory for Marine Mineral Resources, Qingdao National Laboratory for Marine Science and Technology, Qingdao* 266071, *China*
[c] *College of Marine Geo-Science, Ocean University of China, Qingdao* 266100, *China*
[d] *Geophysical Exploration Academy of China Metallurgical Geology Bureau, Baoding*, 071051, *China*

ARTICLE INFO

*Article history:*
Received 15 October 2018
Received in revised form 30 November 2018
Accepted 7 December 2018
Available online 8 January 2019

*Keywords:*
Southern Yellow Sea
Potential geological hazards
Buried paleo channels
Single-channel seismic
Active faults

ABSTRACT

Engineering construction actively occurs in coastal zones, and these areas have numerous potential geological hazard factors. Since 2009, the development of geological surveys in sea areas has promoted extensive geophysical surveys in Qingdao offshore. In the present study, the types and distribution of potential geological hazard factors were systematically revealed using sub-bottom profile data, side-scan sonar data, and single-channel seismic data, among others. Based on previous research findings, the potential geological hazard factors are classified, and control factors in Qingdao offshore are discussed. The research results show that the primary potential geological hazards include active faults, buried paleo channels, shallow gas, irregular bedrock, eroded gullies, estuary deltas, tidal sand ridges, and seawater intrusion. In addition, neotectonic movement, sea level changes and sedimentary dynamic processes were the main factors that affected the distribution of geological hazards in Qingdao offshore.

©2019 China Geology Editorial Office.

## 1. Introduction

Marine geological hazards refer to various geological conditions or geological phenomena that directly damage or have a potential influence over the construction of marine projects and safety of marine engineering structures. The research objects of marine geological hazard studies are factors that cause and promote the occurrence of geological disasters as well as the development mechanisms and distribution patterns of geological disasters (Huang QF et al., 1993; Zhang ZZ et al., 2007; Li F et al., 1998; Feng ZQ et al., 1996). In the 1980s, China and the US jointly surveyed the Yellow River estuary and discovered that hazardous phenomena, such as submarine landslides and diapirs, were widely distributed in the Yellow River Delta (Prior DB et al., 1986). Based on remote sensing, sounding and sub-bottom profile data, various types of potential geological hazards were observed, such as shallow gas, active faults, submarine landslides, diapirs and paleochannels, which were widely distributed in the Yellow River Delta area (Zhou LY et al., 2004). Numerous researchers (Li F et al., 1991a; Li XS et al., 2002; Yu ZY et al., 1998; Zhan WH et al., 1995; Gu ZF et al., 2006; Shi WB et al., 1986) have studied the types and distribution patterns of geological hazards in the South Yellow Sea and discovered that geological hazardous phenomena, such as buried paleochannels (Qin YS. et al., 1987; Li F et al., 1991b) and buried paleo deltas (Li F et al., 1998), were widely distributed in the offshore sea area of the South Yellow Sea.

Qingdao offshore is located in the western sea area of the South Yellow Sea, and the deepest location of this area is at the Jiaozhou Bay mouth, which has a water depth of 64 m below sea level. Its located east of the Tanlu Fault is situated at the juncture between the North China Plate and Yangtze Plate. The Jiaolai Basin and Qianliyan Uplift are the main tectonic units in the study area; the fault system is relatively developed, and the main faults are NNE trending and NW trending (Zhang Y et al., 2013). The main bottom sediment types in Qingdao offshore are silt and sandy silt. According to the literature, coastal currents and Yellow Sea circulation are the main current systems in, which form a mesoscale

* Corresponding author: *E-mail address*: 353511791@qq.com (Ze Ning); qimgzy@163.com (Yong Zhang).

doi:10.31035/cg2018074
2096-5192/© 2019 China Geology Editorial Office.

Copyright 2019 Editorial Office of China Geology. Publishing services provided by Elsevier B.V. on behalf of KeAi.
This is an open access article under the CC BY-NC-ND License (http://creativecommons.org/licenses/by-nc-nd/ ).

anticyclonic vortex under the influence of the winter monsoon (Xu DY and Zhao BR, 1999). In recent years, investigations and studies have been conducted in the offshore sea area of Qingdao and related research articles have been published. Based on the measured digital sonar data, Zhao TH et al. (2005) described the submarine landform of the offshore sea area of Qingdao; Zhao indicated that scour troughs, tidal sand ridges, eroded depressions, subaqueous shore slopes and tidal flats were the main landform types in the Qianhai area of the Jiaozhou Bay and related to strong ocean currents and weak waves, whereas scour troughs and subaqueous shore slopes were the main landform types in the area between the Jiaozhou Bay mouth and Laoshantou. Wang HX et al. (2005) stated that the restrictive hazardous factors in the offshore sea area of the Shandong Peninsula, including paleo channels, paleo-tidal creeks, submarine swells, diapirs and shallow unconformable surfaces, were related to the distribution and cause of each type of geological hazard. Zhang YM et al. (2012) described the morphologies and causes of the submarine landslides in the Laoshantou sea area of Qingdao. Based on multi-beam sounding, sub-bottom profiles and side-scan sonar data, they discovered landslide factors such as landslide mass and its shear plane and drag bedding and suggested that relatively large-scale landslides had occurred in this area; in addition, they found that the translational landslides were formed because of the influence of the terrain of Laoshantou. Factors for geological hazards, such as submarine sand waves, tidal sand bodies, deep-water depressions and faults, have developed in the Jiaozhou Bay mouth area (Bian SH et al., 2006). Wang W et al. (2006) suggested that the Jiaozhou Bay has mainly been affected by sea level changes, climate and regional geology in historical periods, and insignificant overall changes occurred in the Jiaozhou Bay; however, human activities in modern times have resulted in the aggravation of coastal erosion in the Jiaozhou Bay.

In summary, previous studies were all based on sub-bottom profiles and side-scan sonar data. Since 2009, the development of geological surveys for marine areas have promoted extensive geophysical surveys and sample collections in the southern offshore sea area of the Shandong peninsula; in particular, single-channel seismographs have been employed, and a series of potential hazardous geological factors generated since the Neogene have been discovered. In the present study, the above data were used to systematically summarize and determine the hazardous factors in the Qingdao offshore, such as buried paleochannels, irregular bedrock surfaces, active faults and shallow gas. These factors pose potential risks to marine engineering construction.

## 2. Methods

The sub-bottom profile (2800 km) data, side-scan sonar (1100 km) data and high-resolution single-channel seismic (2800 km) data acquired by the Qingdao Institute of Marine Geology in the offshore sea area of Qingdao are used in the present study. Fig. 1 shows the locations of the survey lines and typical profiles in detail.

The sub-bottom profile data were collected in July 2009 using a digital sub-bottom profiling system manufactured by Applied Acoustic Engineering Limited (SBP; AAE, UK) (excitation energy: 300 J; firing interval: 480 ms; frequency of the band-pass filter: 320–2000 $H_2$; measuring range: 160 ms; depth of penetration≥50 m). The single-channel seismic data were collected using a DELPH Seismic collection system, which measured signals of high frequency-rich energy in a wide frequency band (mainly between 20 –900 Hz). The sampling rate was relatively high, and the single-channel seismic data were high-resolution. The burial depth of the bedrock in the offshore sea area was relatively shallow. All other effective reflections were generally greater than 500 –600 ms, and the depth of penetration was greater than 300 m. Therefore, the seismic data, which were collected in July 2011, could satisfactorily reveal the strata formed since the Neogene. The side-scan sonar data were collected at a low frequency (120 kHz) in June 2011 using an Edgetech 4200 side-scan sonar system (measuring range: 100 –150 m; time varying gain (TVG): 19 dB; gain: 7 dB; release length of the towline: 20–40 m; underwater depth of the towfish: 6–10 m).

## 3. Results and discussion

### *3.1. Classification of potential geological hazard types*

Currently, a unified standard has not been established for the classification of geological hazard types. The present study applied previous classifications and research findings of geological hazards (Liu XQ et al., 2006) to determine the geological hazard types, and the geological hazard factors in the Qingdao offshore were classified into five major types based on the causes of these geological hazard factors and states of the geological bodies; the dominant classification factors were as follows: tectonism, hydrodynamism, special phase sedimentation, bearing capacity difference and groundwater changes (Table 1).

### *3.2. Distribution characteristics of the potential geological hazard factors and control factors*

The environmental geology of the offshore sea area of Qingdao is complex, and the potential geological hazard factors primarily include active faults, tidal sand ridges, shallow gas, irregular bedrock, erosion gullies, buried incised valleys, estuary deltas, active faults, and seawater intrusion Fig. 2 shows the distribution of geological hazards.

#### *3.2.1. Active faults*

The depth of the strata revealed by the single-channel seismic data is greater than 300 m; therefore, these single-channel seismic data can satisfactorily reveal the strata formed since the Neogene and explain the active faults. When the seismic reflection wave group is faulted, the pull-down of the reflection wave group and fault diffraction waves can both be used as the identification marks for faults. Based on the single-channel seismic data, three NE-trending active faults with different lengths of extension. The longest NE-trending active fault is 70 km long and located west of the Qianliyan

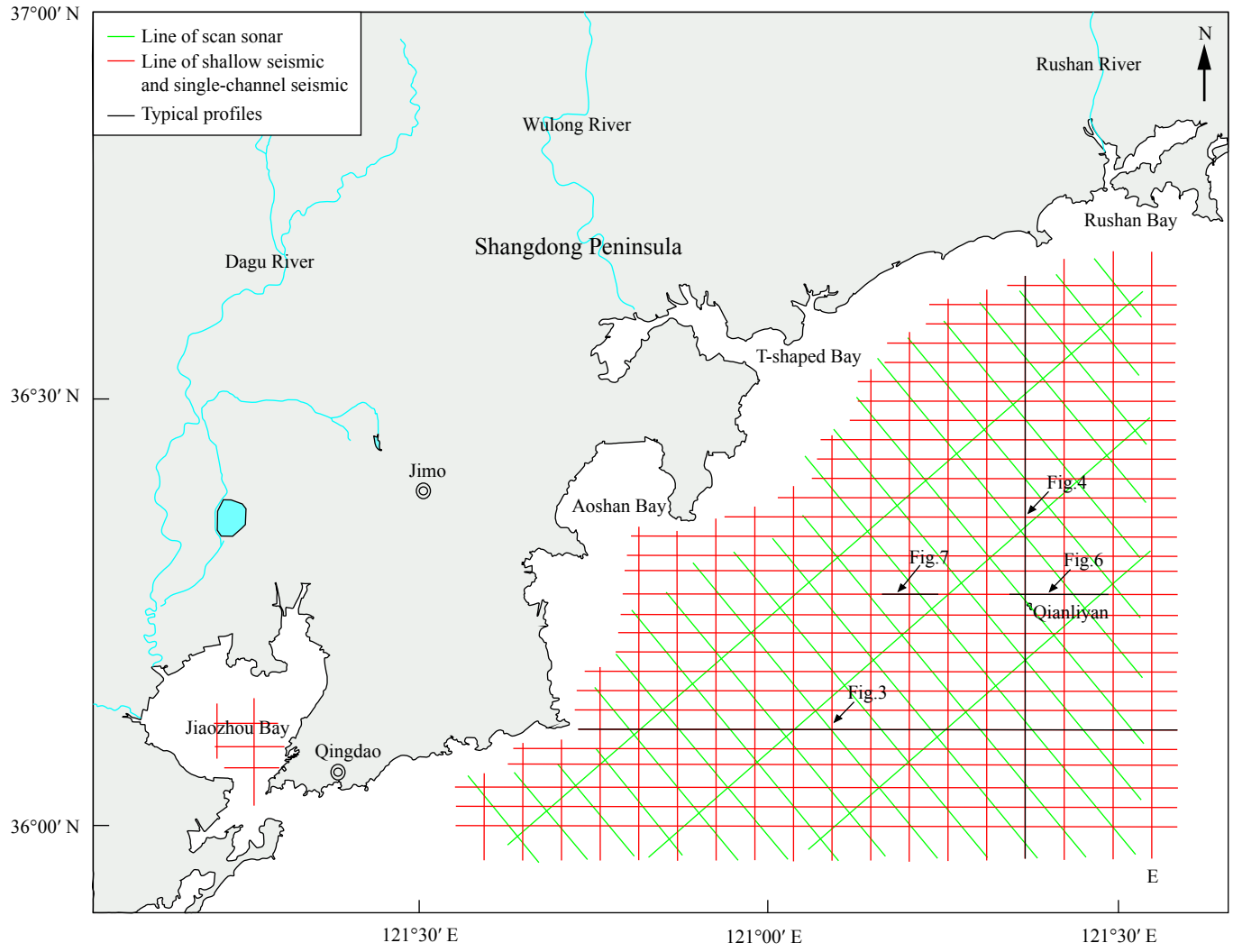


**Fig. 1.** Distribution of the seismic line and locations of typical profiles in Qingdao offshore, China.

Island. The other two active faults are 10 km and 15 km long. The fault throws of all three faults are not large, and the faults are mostly high angle vertical faults. Most of the faults have penetrated the bottom boundary layers of the Neogene and Quaternary to reach the middle Pleistocene from the bottom. A small number of faults have continued to penetrate the late Pleistocene and Holocene to reach the seabed from the middle Pleistocene (Fig. 3, Fig. 4).

**Table 1. Classification of potential geological hazardous factors.**

| Causes | Potential geological hazardous factors |
|---|---|
| Tectonism | Active faults and earthquakes |
| Hydrodynamism | Eroded coasts, silted coasts, underwater sand slopes, tidal sand ridges, tidal scour troughs, submarine erosion gullies, underwater deltas, tidal deltas |
| Special phase sedimentation | Diapirs and shallow gas |
| Bearing capacity difference | Buried paleochannels and shallow buried bedrock |
| Groundwater changes | Seawater intrusion |

*3.2.2. Shallow gas*

The two main causes of submarine shallow gas are biological and thermal, and they are both attributed to organic matter. Shallow gas is manifested as canopy reflection, curtain reflection, turbid reflection, white noise,“bright spots”, mud diapirs (Fig. 4) and gas chimneys in geophysical images. In the present study, the sub-bottom profile and single-channel seismic data indicate that shallow gas is shallowly distributed in the vertical direction, with the top boundary approximately 10 m from the seabed. In addition, shallow gas is concentrated in five areas and generally distributed in layers in large areas of the same stratum. Shallow gas is mainly distributed around the paleochannels formed at the Dingzi Bay mouth and located on the same stratum as the paleochannel sediments of the period. The submarine paleochannel sediments primarily contained terrigenous clastics that were rich in organic matter, which was primarily humic and formed the shallow gas reserve through biodegradation. The occurrence of shallow gas is extremely hazardous to pile foundations, particularly bored pile construction, and it results in submarine soil layer swelling, which increases the compressibility of the soil layer and

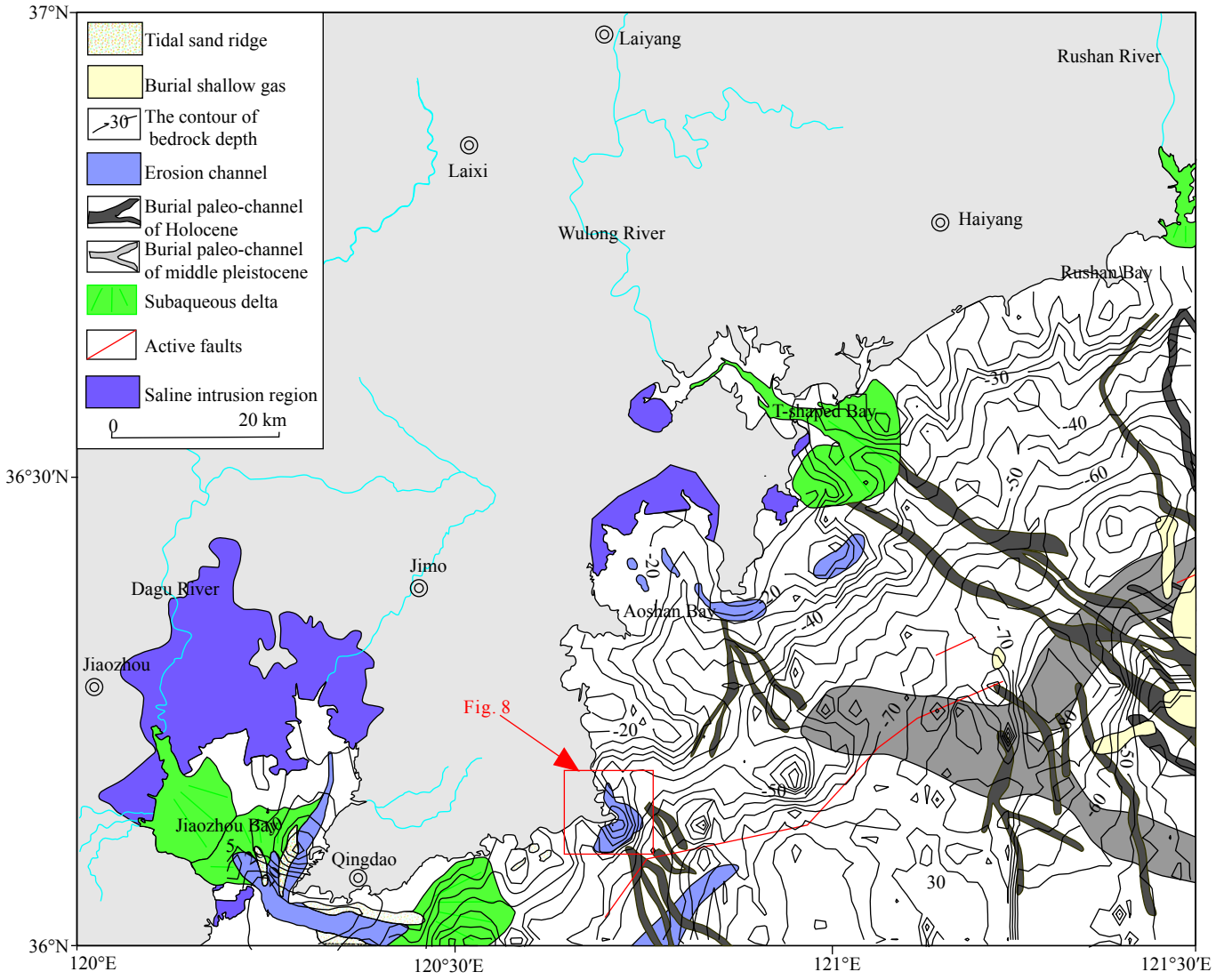


**Fig. 2.** Distribution of the geological hazards in Qingdao offshore, China.

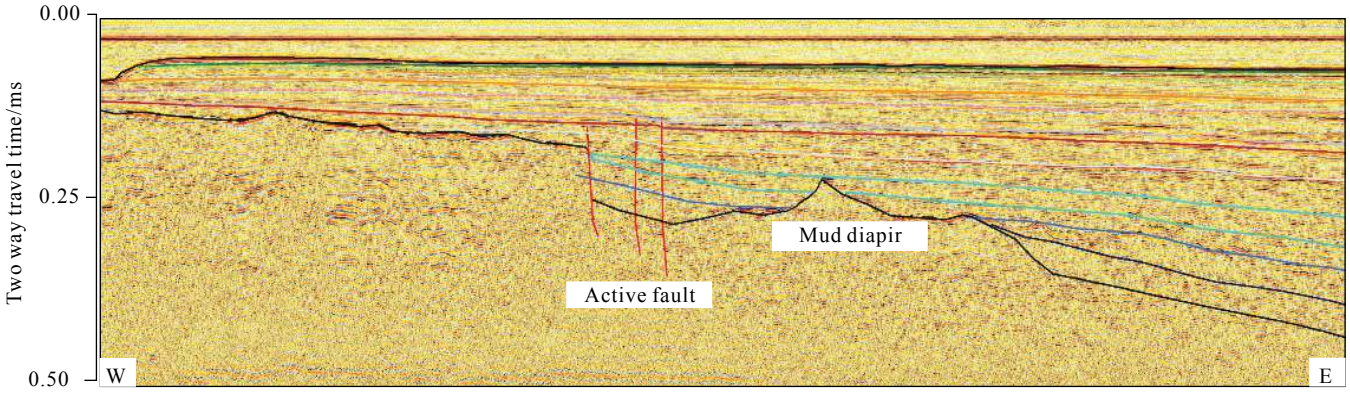


**Fig. 3.** Hazard factors revealed by the single-channel seismic data-Z24 survey line.

reduces its shear strength (Zhao YX et al., 2013). Thus, well blowouts occur when the pressure is sufficiently high during bored pile construction (Whelan NT et al., 1977), which is often detrimental to engineering construction.

*3.2.3. Buried incised valleys*

The distribution of buried paleochannels was mainly controlled by sea level changes caused by global climate change. Since the Quaternary, the alternation of cold and

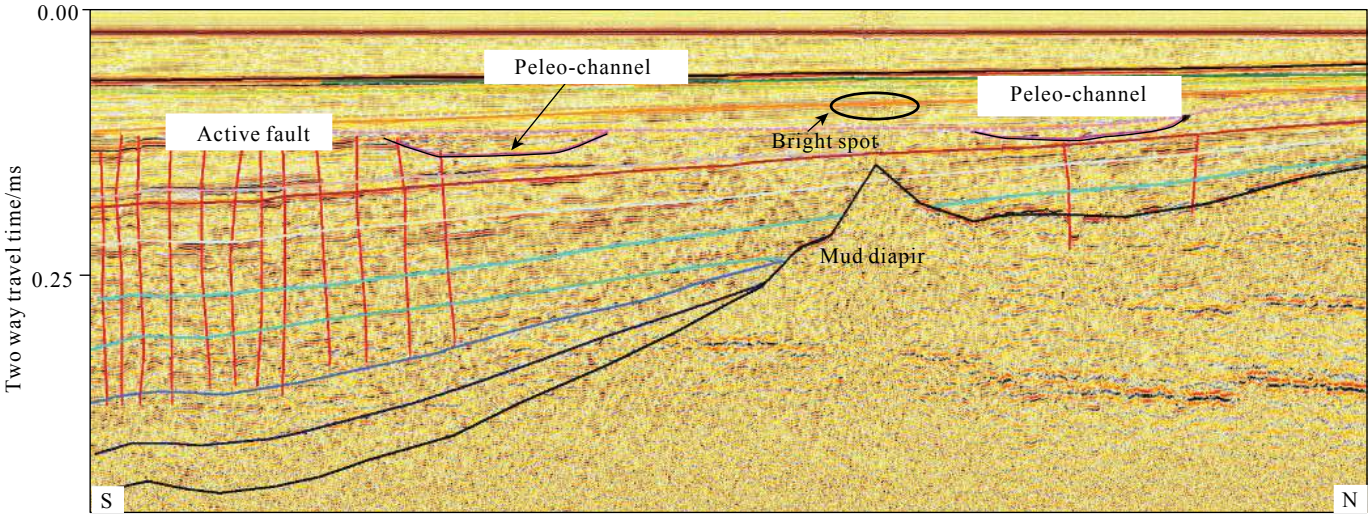


**Fig. 4.** Hazard factors revealed by the single-channel seismic data - L2 survey line.

warm climates has resulted in multiple sea level changes (Sun TC et al., 1977), and multiple land-sea changes have occurred in the Yellow Sea. Because of alternations of rising and falling sea level during glacial and interglacial periods, land-sea changes frequently occurred in the South Yellow Sea. The sea level generally fell during glacial periods, with the sea level of China once falling by 130–160 m (Zhang MH et al., 1998). Globally, there have been three high sea level periods and two low sea level periods since the late Pleistocene. Chappell J et al. (1996) plotted the variation curve of sea level covering the period since 140 ka based on the coral reef terraces and oxygen isotopic profile of a hole drilled on the Papua New Guinea peninsula (Fig. 5). Based on the analysis of the sub-bottom profile data and drill hole data obtained in the Qingdao offshore, the sea level of the shelf sea of the Yellow Sea has been found to have similarly fluctuated since the late Pleistocene. However, because of differences in location, the fluctuation of sea level of the shelf sea of the Yellow Sea might have occurred at different times compared with the fluctuations at other locations. In addition, the extent to which the sea level of the shelf sea of the Yellow Sea rose or fell might also have been different from the sea levels at other locations. In the late Late Pleistocene (approximately 25–15 ka BP), the climate rapidly turned cold, and the sea level of the shelf sea of the Yellow Sea fell significantly so that the continental shelf of the Yellow Sea was gradually subaerially exposed and became land. During the Pleniglacial period, the sea level was 120–135 m lower than present-day sea level (Qin YS et al., 1987). The Dagu River, Baisha River and Moshui River, which developed in the Jiaozhou Bay, and Wulong River and Rushan River, which developed on land surrounded by the Dingzi Bay, Rushan Bay and Aoshan Bay, flowed along the trend and converged at the center of the bay and sea to form river channels of various scales. After the Last Glacial Maximum, the global climate began to warm, and sea level began to rise. At 8500 a.BP, marine transgressions reached their maximum level and the sea level was close to the present-day level. After seawater intrusion, several of the previously formed river channels became tidal channels; which were filled at certain locations (Fig. 5).

The sub-bottom profile data (Fig. 6) and single-channel seismic data (Fig. 4) show that the buried paleochannels that formed in two different periods (Holocene and middle Pleistocene) are distributed. Among the buried paleochannels formed in the late Quaternary, there are four relatively large paleochannels that are mainly distributed in the sea areas near Rushankou, the Dingzi Bay, Aoshan Bay and Laoshan Mountain. Paleochannels formed in the middle Pleistocene are relatively wide and mainly distributed in the sea area east of Laoshan Mountain, and the SEE-trending main channel branches into two channels: one is NE-trending and the other is SE-trending. The two channels branch and flow away along the Qianliyan Island, and the SE-trending channel branches again into two channels, with a maximum buried depth of the paleochannel of 140 m. There are large variations in the incised depths and widths of the paleochannels that were formed in the Holocene. The maximum incised depth can reach over 35 m, the widths primarily range from 0.5–2 km, and the maximum width can reach 4 km. Most of the sediments in the paleochannels have large porosities and are complex, and there are relatively large variations in the particle size composition, degree of sorting and compressive and shear strength in the horizontal direction. Under a cover load, the sediments may easily result in local collapses, and

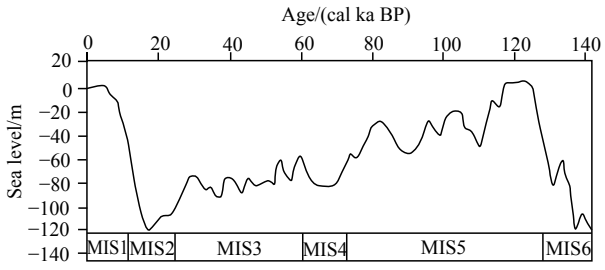


**Fig. 5.** Variation curve of the sea level of the South Yellow Sea since 140 ka BP (after Sun TC et al., 1977).

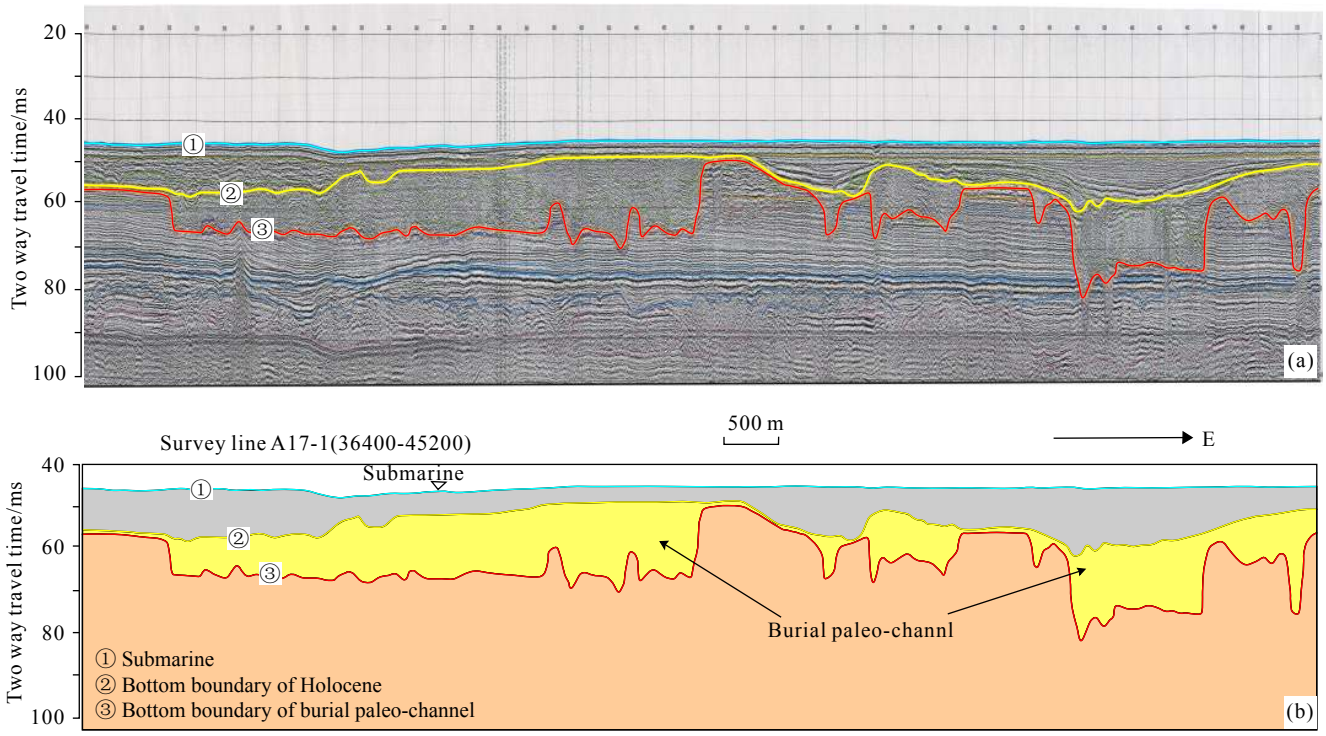


**Fig. 6.** Buried paleochannels revealed by the sub-bottom profile data (Fig. 1. for locations).

the non-uniform deposition of the sediments may result in unstable foundations. Therefore, it is necessary to avoid paleochannels or take measures to reinforce foundations when designing engineering projects.

*3.2.4. Irregular bedrock*

Irregular bedrock is manifested as excessively varying degrees of bedrock relief, such as bedrock that protrudes irregularly or caves in suddenly. Irregular bedrock is often indicated by strong reflection or lateral reflection in sub-bottom profile recordings. In seismic recordings, irregular bedrock undulates irregularly, and the protuberances of bedrock surfaces are tip shaped and saw-tooth shaped (Fig. 7). The reflection inside irregular bedrock is random and obscure. Based on the tracking of strong reflection interfaces shown in the sub-bottom profile recordings, the morphologies and burial depths of the bedrock surfaces and range of irregular bedrock are easily determined. The shallow-buried irregular bedrock is mainly concentrated in the coastal areas and near each island, and the burial depths of the shallow-buried irregular bedrock vary relatively significantly in a range of 0–100 m. The sub-bottom profile data show that the irregular bedrock within the range of Qingdao is mainly concentrated in six areas: near Qianliyan, near Dingzi Bay, eastern and southern Laoshan Mountain, near Nandao Island and Jiaozhou Bay. The bedrock within Jiaozhou Bay is mainly distributed in the areas near Hongdao Island and the bay mouth. Overall, the depths of the bedrock surfaces gradually become deeper in the direction from the shores to shallow sea. Irregular bedrock surfaces are mainly distributed in the offshore sea area or areas close to reefs and islands. Irregular bedrock compose part of the sea island rock bodies that have extended toward the sea. The bedrock in the areas close to the islands (Tianheng Island, Qianliyan Island, etc.) and at the tidal inlet of the Jiaozhou Bay mouth is not covered with sediment and is exposed to the seabed.

*3.2.5. Erosion gullies*

Submarine erosion gullies were formed from the interaction between the terrain and tidal currents, and they are often seen in areas with strong hydrodynamic forces and a varied terrain. The Yellow Sea coastal currents provided the hydrodynamic conditions for the formation of submarine erosion gullies, which were shown by side-scan data show to be distributed in the offshore sea area of Qingdao; in addition, more erosion gullies occurred in the south than in the north. Erosion gullies are widely distributed in the Jiaozhou Bay mouth, southern offshore sea area of Laoshantou and Aoshan Bay mouth. According to the side-scan data, the erosion gullies in the Qingdao offshore are mainly distributed in the Jiaozhou Bay mouth, area near the Aoshan Bay mouth and southern offshore sea area of Laoshantou. Because of the "narrow" effect of the Jiaozhou Bay mouth gate, the bottom was scoured more intensively by tidal currents, which resulted in the formation of gullies because of erosion at the bay mouth. The scour pit in the main tidal channel at the Jiaozhou Bay mouth is as deep as 64 m, there are steep slopes on the two sides, and the seabed is composed of bedrock and formed by intensive erosion from tidal currents caused by the main tidal channel changing its course near the mouth bay. The sedimentary layer in the tidal channel is shallow, and exposed bedrock is observed at several locations. The large-scale

erosion gully formed by tidal currents in the southern offshore sea area of Laoshantou is approximately 7 km long; the maximum width of this erosion gully is approximately 2 km, and the maximum water depth is 53 m. This erosion gully encircles Laoshantou from the north to south to west, forming an inverse L-shape that is fairly consistent with the southern coast of the Laoshan Mountain (Fig. 8). In addition, rock, gravel and shells have accumulated on the seabed, and exposed bedrock is observed at certain locations.

*3.2.6. Tidal sand ridges*

Tidal sand ridges are a type of ridge-shaped sand body that developed on the seabed because of tidal deposition. Tidal sand ridges often develop at estuaries, delta fronts and straits (Swift DJP, 1968; Dalrymple RW et al., 1990). The morphology and location of tidal sand ridges can change under the influence of hydrodynamic and external forces. Coastal currents and Yellow Sea circulation are the main current systems in this area, and they provide the hydrodynamic conditions required for the formation of tidal sand ridges. The tidal sand ridges are mainly distributed at the Jiaozhou Bay mouth and in a southwestern direction from Laoshan Mountain. The tidal sand ridges at the Jiaozhou Bay mouth extend from south to north, and the sand ridges are separated by tidal channels to form a gully-ridge alternating terrain. The sand ridges are composed of coarse and medium-coarse sand. The longest sand ridge is 16 km, and the tidal sand ridges in a southwestern direction from the Laoshan Mountain extend in an east to west direction. Reciprocating tidal currents are the main type of tidal current in the sea area of Jiaozhou Bay, and they exhibit the regular characteristics of semidiurnal tidal currents. When the tide rises, the tidal currents from the open sea enter the bay through the Jiaozhou Bay mouth and then branch because of the influence of shorelines within the bay and submarine terrain. When the tide is at ebb, the tidal currents flow out of the bay through the bay mouth in the direction opposite to the one at which they entered. Because of the restricted entry effect, the speed of the tidal currents at the Jiaozhou Bay mouth is the highest. The speed of the tidal currents gradually decreases as they flow

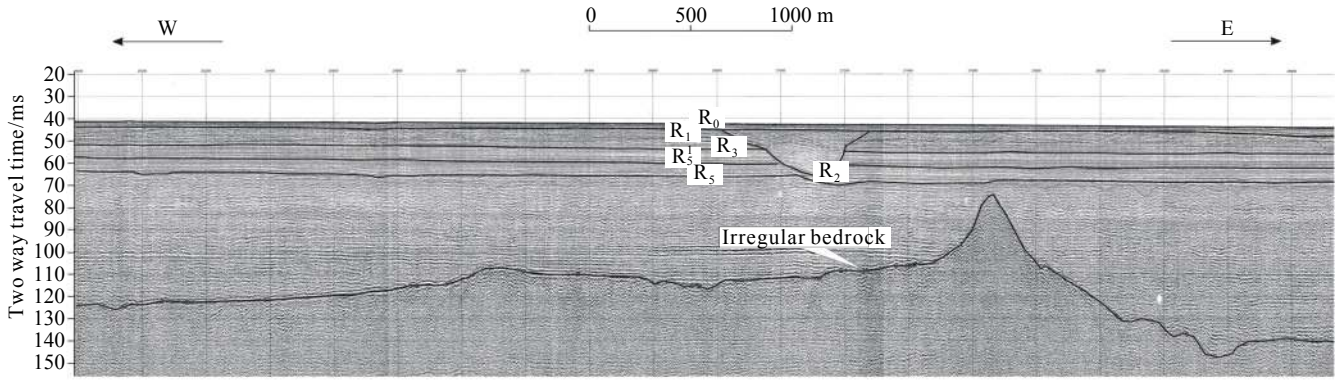


**Fig. 7.** Irregular bedrock revealed by the sub-bottom profile data (Fig. 1 for locations).

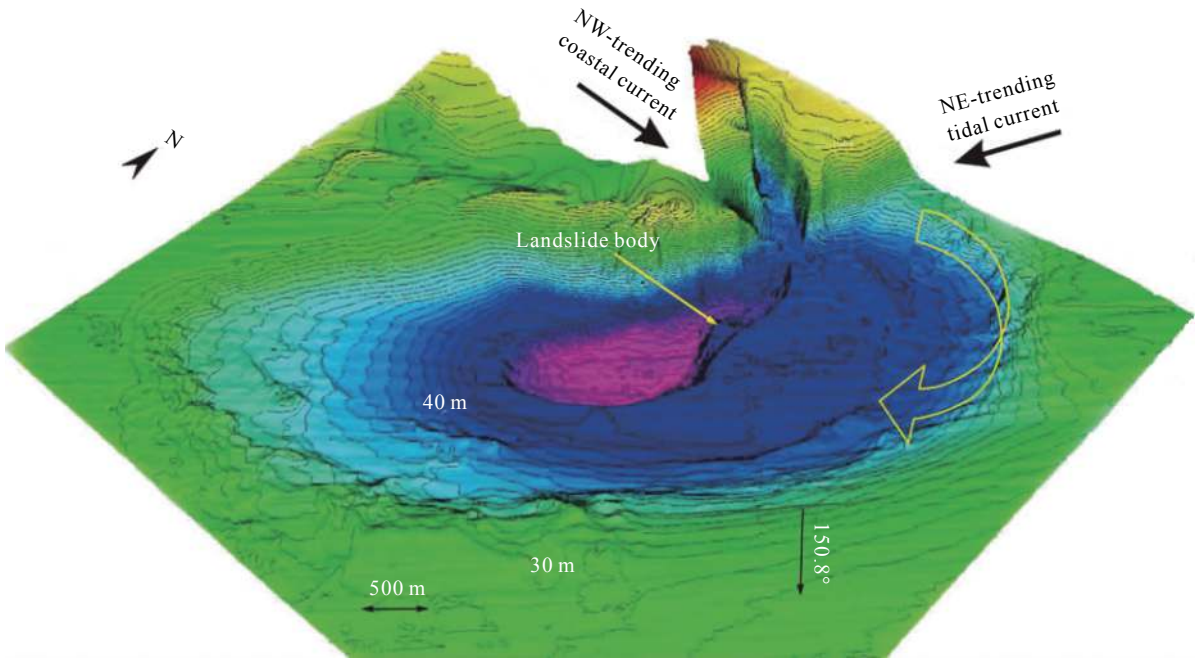


**Fig. 8.** Erosion gullies in the sea area of Laoshantou (after Zhang YM et al., 2012).

into the bay; after reaching the bay top area, the flow direction of the tidal currents begins to diverge, and the speed of the tidal current decreases rapidly. The suspended sand within Jiaozhou Bay is mainly from the bay top area; ebbing tidal currents spreads the suspended sand toward the bay mouth along the shore, where a significant concentration front of suspended sand forms in the northern section of the channel. Therefore, the saddle of the depth contour in Jiaozhou Bay and the northern section of the bay mouth channel are the main locations for the convergence of sand. Thus, three large-scale tidal sand ridges were formed within the bay. Because of the influence of the ebbing tidal currents, line-shaped sand ridges parallel to the main tidal channel developed on the two sides of the main tidal channel.

*3.2.7. Estuary deltas*

Deposition is more significant than erosion in delta areas. When a river is entering the sea, the river currents disperse at the estuary, and their kinetic energy decreases; thus, the sediments carried by the river currents deposit at the estuary, forming a triangle-shaped terrain with the spire facing the inland. Delta sediments often contain organic matter; therefore, natural gas is often accumulated at estuary deltas. In addition, sedimentary particles on delta fronts have small particle sizes, and the slopes of delta fronts are steep; thus, the hydrodynamic forces are active at estuaries, and geological hazards, such as landslides and mudslides, may easily occur. There are three major estuary deltas that are distributed: Dagu River-Yanghe River complex delta, Dingzi Bay estuary delta and Rushan estuary delta. In addition, because of the tidal effect, a flood delta and ebb delta have developed near the tidal channels of Jiaozhou Bay. Because the amount of sediments that rivers carry to the estuary is relatively small and organic matter spreads and is relatively well distributed under marine hydrodynamic forces, the morphology of the delta is not obvious. The sediments carried by the Dagu River are the main material source of Jiaozhou Bay. Because the strength of flooding is higher than the strength of ebbing, the sediments brought by river scouring are not easily transported to the bay. Therefore, these sediments have been deposited successively at the shallow water area near the estuary based on their particle size and density. The Dingzi Bay estuary delta extends in the southeastern direction and has a relatively large distribution area with a relatively smooth surface. The Dingzi Bay estuary delta was formed by the rapid accumulation of sediments brought by the Wulong River to the estuary. The Rushan Bay estuary delta is relatively small and extends from the Rushan Bay mouth in a southern direction.

*3.2.8. Seawater intrusion*

Seawater intrusion in the Qingdao offshore mainly occurs at Jiaozhou Bay, Aoshan Bay and Dingzi Bay (Fig. 2 and Table 2). The seawater intrusion area is approximately 544 km$^2$, and the largest intrusion occurs in the Jiaozhou Bay area (449 km$^2$), which accounts for 82.54% of the total seawater intrusion area within the range of Qingdao. The sea water intrusion area of Aoshan Bay (67 km$^2$) and Dingzi Bay (28 km$^2$) accounts for 12.32% and 5.15% of the total sea water intrusion area in the study area.

**Table 2. Seawater intrusion areas in the Qingdao offshore.**

| Locations | Seawater intrusion areas/km$^2$ | Percentages |
|---|---|---|
| Jiaozhou Bay | 449 | 82.54% |
| Aoshan Bay | 67 | 12.32% |
| Dingzi Bay | 28 | 5.15% |
| Total | 544 | 100% |

## 4. Conclusions

(i) The potential geological hazard factors in the offshore sea area of Qingdao include active faults, buried paleochannels, shallow gas, irregular bedrock, eroded troughs, estuary deltas, and tidal sand ridges; active faults, buried paleochannels and tidal sand ridges are the main geological hazards.

(ii) The Neotectonic movement, sea level changes and sedimentary dynamic processes were the main factors that affected the distribution of geological hazards in Qingdao offshore.

## Acknowledgment

The authors appreciated the Executive Editor-in-Chief Dr. Yang Yan and the anonymous reviewers for their constructive comments that improved the quality for original manuscript. The present study was jointed funded by the National Natural Science Foundation of China (41376079 and 41276060), Marine Geology Survey Project (GZH200900501, DD20160137 and DD20190205) and Foundation of the Shandong Provincial Key Laboratory of Marine Ecology and Environment & Disaster Prevention (201304).

## References

Bian SH, Xia DX, Chen YL, Zhao YX. 2006. The classification characteristics and developing factors of the sandwaves at the mouth of Jiaozhou Bay. Periodical of Ocean University of China, 36(2), 327–330.

Chappell J, Omura A, Esat T, McCulloch M, Pandolfi J, Ota Y, Pillans B. 1996. Reconciliation of late Quaternary sea levels derived from coral terraces at Huon Peninsula with deep sea oxygen isotope records. Earth and Planetary Science Letters, 141(1), 227–236.

Dalrymple RW, Knight RJ, Zaitlin BA, Middleton GV. 1990. Dynamics and Facies model of a macrotidal sand-bar complex, Cobequid Bay-Salmon River Estuary. Sedimentology, 37, 577–612. doi: 10.1111/sed.1990.37.issue-4.

Feng ZQ, Feng WK, Xue WJ, Liu ZH, Chen JR, Li WF. 1996. Evaluation of marine geologic hazards and engineering geological conditions in the northern south China sea. Nanjing: Hehai University press, 87.

Gu ZF, Zhang ZX, Liu HS. 2006. Seismic features of shallow gas in the western area of the Yellow sea. Marine Geology & Quaternary Geology, 26(3), 65–74.

Huang QF, Yan J, Lin GJ, Dong TL, Jiang RH. 1993. Strengthen marine disastrous geological studies and decrease marine engineering

hazard. Marine Geology & Quaternary Geology, 13(4), 99–103.
Li F, Zhang XR, Tang BY. 1998. Atlas of Yellow sea buried paleo-channels and geological hazards. Jinan: Jinan press, pp. 12–20.
Li F, Zhang XR, Meng GL, Han GL. 1998. Buried Paleo-Huanghe River delta in the central southern Yellow sea during the late Pleistocene. Oceanologia et Limnologia Sinica, 29(1), 67–72.
Li F, Yu, JJ, Jiang XH, Yu JD. 1991a. Study on geohazard in the south Yellow sea. Marine Geology & Quaternary Geology, 11(4), 11–23.
Li F, Yu JJ, Jiang XH, Du QS, Song HL. 1991b. Study on buried Paleo-channel system in the south Yellow sea. Oceanologia et Limnologia Sinica, 22(6), 501–508.
Li XS, Liu BH, Zheng YP, Li SZ, Wang KY. 2002. Types and acoustic reflection characteristics of geological hazards in Yellow sea and east China sea. Journal of Ocean University of Qingdao, 32(1), 107–114.
Liu XQ. 2006. Marine coastal environmental geology China seas. Beijing: Ocean Press, 155–229.
Prior DB, Yang ZS, Bornhold BD, Keller GH, Lu NZ, Wiseman WJ, Wright LD, Zhang J. 1986. Active slope failure, sediment collapse, and silt flows on the modern subaqueous Huanghe (Yellow River) delta. Geo-Marine Letters, 6(2), 85–95. doi: 10.1007/BF02281644.
Qin YS. 1987. The East China Sea geology. Beijing: Science Press, 7–86.
Shi WB, Li DP, Wang XC, Zhang ZX. 1986. Shallow seismic surveying in south Huanghai sea and its geological significance. Marine Geology & Quaternary Geology, 6(1), 87–104.
Sun TC, Chou ML, Pan CY. 1977. Quaternary glaciations in China. Acta Geologica Sinica, (2), 101–108.
Swift DJ. 1968. Coastal erosion and transgressive stratigraphy. The Journal of Geology, 76, 44–456.
Wang HX, Guo YG. 2005. Analysis of the main geological hazard types in the coastal and offshore areas of Shandong province. Periodical of Ocean University of China, 35(5), 751–756.
Wang W, Zhang Q, Ji YL. 2006. Evolution and controlling factor of the circuar Jiaozhou Bay coastline. Marine Geology Letters, 22(9), 7–11.
Whelan NT, Colemen JM, Suhayda JN, Roberts HH. 1977. Acoustical penetration and shear strength in gas-charged sediment. Marine Geotechnology, 2, 147–159. doi: 10.1080/10641197709379776.
Xu DY, Zhao BR. 1999. Existential proof and numerical study of a mesoscale anticyclonic eddy in the Qingdao-Shidao offshore. Acta Oceanologica Sinica, 21(2), 19–26.
Yu ZY, Fan SJ, Jin M. 1998. The old Yellow river underwater delta in the north Jiangsu and the seaport building. Acta Geographica Sinica, 53, 158–166.
Zhan WH, Liu YX, Zhong JQ, Lu CB. 1995. Preliminary analysis of the active faults and hazard geology in the south of the south China sea. Marine Geology & Quaternary Geology, 15(3), 1–9.
Zhang MH, Yu HJ. 1998. The paleogeomorphic features of the middle part of the south Yellow sea shelf in the last stage of late Pleistocene. Studia Marina Sinica, (40), 65–77.
Zhang Y, Ren FL, Gong SY, Zhang XR, Lin MM, Liu SS. 2013. Cretaceous stress field of the Muping-Jimo fault belt and its implication for tectonic evolution. Marine Geology & Quaternary Geology, 33(2), 78–85.
Zhang YM, Bi JQ, Sun ST, Shi XW, Xiao CQ. 2012. Sound wave prospecting in the submarine landslip in Laoshantou sea area of Qingdao. Chinese Journal of Engineering Geophysics, 9(2), 170–174.
Zhang ZZ, Gu ZF, Liu XQ, Zhang ZX. 2007. Hazardous geology and marine geologic environmental evolution in the south Yellow sea. Marine Geology & Quaternary Geology, 27(5), 15–22.
Zhao TH, Li C, Cong HW, Chu HX. 2005. Relief type and acoustic characters of inshore seabed along Qingdao. Hydrographic Surveying and Charting, 25(1), 40–43.
Zhao YX, Xu QH, Liu FY, Qin YJ, Wu C, Chen LJ, Cui JH. 2013. Progresses of palaeochannel studies in China in the past 20 years. Progress in Geography, 32(1), 3–19.
Zhou LY, Liu J, Liu XQ, Li GX, Chen ZX. 2004. Coastal and marine geo-hazards in the modern Yellow river delta. Marine Geology & Quaternary Geology, 24(3), 19–27.